

Effects of the Chodura sheath on tungsten ionization and emission in tokamak divertors

J. Guterl¹ | C. Johnson² | D. Ennis² | S. Loche² | P. Snyder¹

¹General Atomics, San Diego, California, USA

²Auburn University, Auburn, Alabama, USA

Correspondence

J. Guterl, General Atomics, San Diego, CA, USA.

Email: guterlj@fusion.gat.com

Funding information

U.S. Department of Energy, DE-FG02-95ER54309, DE-SC0018423

Abstract

The decay of the electric potential in the sheath region in tokamak divertors occurs on a scale length on the order of the main ion gyroradius (Chodura sheath) due to magnetic field lines intersecting the divertor plates at grazing incidence. As a consequence, high-Z impurities like tungsten ionize within the sheath region in attached plasma conditions. The modification of the electron distribution in the sheath region must thus be taken into account to accurately model ionization and emission of impurities within the sheath region. To that end, an analytical expression of the distribution of the vertical ionization path for impurities sputtered from divertor plasma-facing components is derived. This expression is then used to estimate the fraction of neutral impurities ionizing within the sheath and the average vertical ionization path, and to derive an effective SXB (the number of ionizations per emitted photon) coefficient which includes the effects of the variation of the electron distribution in the sheath region. These results are applied to tungsten impurities sputtered from divertor plates. It is shown that the SXB coefficient for neutral tungsten is significantly reduced in high-density attached divertor plasma conditions ($n_e \gtrsim 5 \times 10^{13} \text{ cm}^{-3}$) because of the ionization of neutral tungsten well within the sheath region.

KEYWORDS

Chodura sheath, divertor, SXB coefficients, tungsten erosion

1 | INTRODUCTION

Divertors in International Thermonuclear Experimental Reactor (ITER) and other future fusion reactors will be made of tungsten plasma-facing components (PFCs),^[1] and will be operated in partially detached plasma and perhaps with small edge localized mode. For those plasma regimes, the erosion of tungsten PFCs may significantly reduce the PFCs lifetime and deteriorate plasma performance due to the contamination of the core plasma by tungsten impurity. Accurate predictions of tungsten erosion in boundary plasma are thus required to design and operate divertor in future fusion reactors. Furthermore, reliable in situ experimental measurements of tungsten erosion during plasma operations must be developed to validate predictive models of tungsten net erosion and monitor the evolution of tungsten sources in divertor during long plasma pulses.

Divertors in present tokamaks and future fusion reactors are characterized by a tilted magnetic field intersecting divertor PFCs surfaces at very shallow angle below 5°. This magnetic field at shallow incidence strongly impacts the electric sheath through a large decay of the electric potential in the magnetic presheath, and conversely a small decay

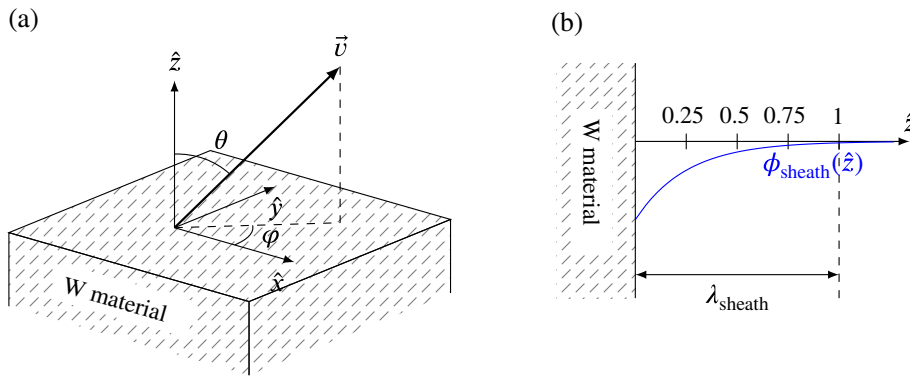


FIGURE 1 (a) Velocity of sputtered neutral impurity from a flat material surface in spherical coordinates. (b) Electric potential in the sheath ϕ_{sheath} (Equation 12)

of the electric potential in the Debye sheath,^[2,3] leading to the formation of a Chodura sheath. The decay of the electric potential in the sheath thus occurs over a scale length much larger than the Debye length, and the width of the sheath region is of the order of the main ion Larmor radius. As pointed out by Fussmann,^[4] such a wide electric sheath may affect the ionization of sputtered impurities due to the variations of the electron distribution in the sheath. Whereas these effects are noticeably negligible for low-Z impurities, such as carbon or beryllium which ionize outside of the sheath, the ionization of high-Z impurities like tungsten can occur within the sheath region, and thus affects tungsten emission as well as tungsten prompt redeposition.

This paper addresses specifically the ionization of neutral tungsten impurities within the sheath region and its consequence on the subsequent impurity emissivity. Effects on impurity prompt redeposition will be discussed elsewhere. First, an analytical expression of the distribution of the vertical ionization path is derived in Section 2, and it is used to estimate the fraction of neutral impurity which ionized within the sheath and the average vertical ionization path. Using these results, a new expression of the SXB coefficient (the number of ionization events per emitted photon^[5]) is proposed in Section 3 to consider the effects of impurity ionization within the sheath region. These results are then applied in Sections 4 and 5 to tungsten impurities. It is shown that a large fraction of neutral tungsten is ionized well inside the sheath region in high-density attached plasma divertor conditions ($n_e > 10^{14} \text{ cm}^{-3}$), and that the effective SXB coefficient is consequently strongly reduced.

2 | EFFECTS OF THE ELECTRIC SHEATH ON THE IONIZATION OF SPUTTERED NEUTRAL IMPURITIES

We consider in this work impurities of mass M physically sputtered from a flat material surface located at $z = 0$ at the velocity v , the polar angle θ , and the azimuthal angle φ (Figure 1a). The kinetic energy of plasma species impinging on material surface and inducing physical sputtering is assumed to be sufficiently large such that the velocity distribution of sputtered neutral impurity can be described as the convolution of a cosine polar angular distribution f_θ , a uniform azimuthal angular distribution $f_\varphi(\varphi)$ and a Thompson energy distribution f_{Thompson} .^[6]

Trajectories of the neutral tungsten particles emitted from the divertor material surface are assumed to be ballistic until the first ionization event, that is, collisions of sputtered neutral impurities with neutral and charged plasma particles are negligible. The variations of the electron density and temperature along the material surface are ignored, that is, plasma conditions are considered uniform along the material surface. In a tokamak divertor configuration, the ionization mean-free path of neutral impurities emitted from the surface is thus assumed to be smaller than the radial variations of the divertor plasma conditions. Consequently, we only consider in this work the effects of the variations of the electron density and temperature in the sheath along the z direction on the ionization of sputtered impurity. These effects are modelled by the dependence of the vertical ionization path of sputtered neutral impurity $\hat{\lambda}_{\text{iz}} = \frac{\lambda_{\text{iz}}}{\lambda_{\text{sheath}}}$ on the distance \hat{z} from the plate. In this work, the distances are normalized to the width of the sheath region λ_{sheath} (Figure 1b).

Following the standard description of test particle collisions with background plasma particles,^[7] the probability density function f_{iz} of the vertical distance \hat{z}_{iz} from the material surface, at which neutral impurities emitted from the material surface at $\hat{z} = 0$ are ionized, is given by

$$f_{\text{iz}}(\hat{z}_{\text{iz}}) = \frac{1}{\hat{\lambda}_{\text{iz}}(\hat{z}_{\text{iz}})} e^{-\int_0^{\hat{z}_{\text{iz}}} \frac{1}{\hat{\lambda}_{\text{iz}}(\hat{z})} d\hat{z}}. \quad (1)$$

The trajectory of neutral impurities sputtered from material at the velocity v , the polar angle θ , and the azimuthal angle φ is ballistic, so that

$$\hat{\lambda}_{iz}(\hat{z}) = \frac{v \cos \theta}{S_{iz}(\hat{z}) n_e(\hat{z}) \lambda_{\text{sheath}}}, \quad (2)$$

where n_e is the electron density and S_{iz} is the ionization coefficient of sputtered neutral impurities defined by

$$S_{iz}(\hat{z}) = \frac{\int_0^\infty \sigma_{iz}(v_e) v_e f_e(v_e, \hat{z}) dv_e}{n_e(\hat{z})}, \quad (3)$$

$f(v_e, \hat{z})$ is the electron velocity distribution with $\int_0^\infty f_e(v_e, \hat{z}) dv_e = n_e(\hat{z})$. The velocity of sputtered impurities is assumed to be much smaller than the thermal velocity of the electrons ($v \ll \sqrt{\frac{T_e}{m_e}}$) and is thus ignored in expression (3). The ionization rate of sputtered neutral impurity can be expressed as a function of the ionization rate of neutral impurity at the entrance of the sheath, i.e.

$$S_{iz}(\hat{z}) n_e(\hat{z}) = \underbrace{S_{iz,p} n_{e,p}}_{v_{iz,p}} \delta_{iz}(\hat{z}), \quad (4)$$

where the subscript p indicates the values at the entrance of the sheath ($\hat{z} = 1$). The function δ_{iz} is strictly positive and represents the effects of the variation of f_e along the sheath region on the ionization rate, and thus includes in all generality variations of both T_e and n_e . The variations of the electron velocity distribution out of the sheath region is ignored ($\delta_{iz}(\hat{z}_{iz} \geq 1) \approx 1$).

Normalizing the impurity velocity by $\hat{v} = \frac{v}{\lambda_{\text{sheath}} v_{iz,p}}$ and using relationships (2) and (4), expression (1) can be integrated over the angular distributions f_θ and f_ϕ , and over the Thompson energy distribution f_{Thomson} , which reads in the velocity space

$$f_{\text{Thomson}}(\hat{v}) \propto \frac{\hat{v}^3}{(\hat{v}^2 + \hat{v}_b^2)^3} \left(1 - \sqrt{\frac{1 + \left(\frac{\hat{v}}{\hat{v}_b}\right)^2}{1 + \xi_c}} \right), \quad (5)$$

where $\hat{v}_b = \frac{\sqrt{2E_b}}{M} \frac{1}{v_{iz,p} \lambda_{\text{sheath}}}$ is the characteristic velocity of sputtered particles and $\xi_c = \frac{E_{\text{cutoff}}}{E_b}$ is the maximum energy E_{cutoff} at which impurities are sputtered relative to the surface binding energy E_b . The integration of expression (1) leads to the distribution g_{iz} of \hat{z}_{iz} for neutral impurities physically sputtered from divertor plates:

$$g_{iz}(\hat{z}_{iz}) = \frac{d\eta_b(\hat{z}_{iz})}{d\hat{z}_{iz}} \Upsilon_{\xi_c}(\eta_b(\hat{z}_{iz})), \quad (6)$$

where $\eta_b(\hat{z}_{iz}) = \frac{\int_0^{\hat{z}_{iz}} \delta_{iz}(\hat{z}) d\hat{z}}{\hat{v}_b}$ is the effective ionization time. The function Υ_{ξ_c} is defined by

$$\Upsilon_{\xi_c}(\eta_b) = \frac{2}{\eta_b} \frac{\int_{\frac{\eta_b}{\sqrt{\xi_c}}}^{\infty} \frac{\eta^2 (e^{-\eta} - \eta \Gamma_{\text{inc}}(0, \eta))}{\left(1 + \frac{\eta^2}{\eta_b^2}\right)^3} \left(1 - \frac{\eta}{\eta_b} \sqrt{\frac{1 + \frac{\eta^2}{\eta_b^2}}{1 + \xi_c}}\right) d\eta}{\int_{\frac{\eta_b}{\sqrt{\xi_c}}}^{\infty} \frac{\eta}{\left(1 + \frac{\eta^2}{\eta_b^2}\right)^3} \left(1 - \frac{\eta}{\eta_b} \sqrt{\frac{1 + \frac{\eta^2}{\eta_b^2}}{1 + \xi_c}}\right) d\eta}, \quad (7)$$

where Γ_{inc} is the incomplete Gamma function.^[8] Tabulated values of Υ_{ξ_c} are provided as supplemental material.

Using Expressions (6) and (7), the fraction χ_{sheath} of physically sputtered neutral impurities ionized within the sheath region ($0 \leq \hat{z} \leq 1$) can be simply expressed as

$$\chi_{\text{sheath}} = \int_0^1 g_{iz}(\hat{z}_{iz}) d\hat{z}_{iz} = \int_0^{\hat{\lambda}_{iz}^{-1}} \Upsilon_{\xi_c}(\tilde{\eta}) d\tilde{\eta}, \quad (8)$$

where $\hat{\lambda}_{iz,b} = \frac{\hat{v}_b}{\int_0^1 \delta_{iz}(\hat{z}) d\hat{z}}$ corresponds to the characteristic ionization mean-free path \hat{v}_b corrected with the variation of the electron velocity distribution in the sheath region. Similarly, the average vertical ionization path $\bar{\lambda}_{iz}$ reads

$$\bar{\lambda}_{iz} = \int_0^\infty \hat{z}_{iz} g_{iz}(\hat{z}_{iz}) d\hat{z}_{iz} = \int_0^\infty \Phi_b(\tilde{\eta}) \Upsilon_{\xi_c}(\tilde{\eta}) d\tilde{\eta}, \quad (9)$$

where Φ_b is the inverse function of $\eta_b(\hat{z})$ and is the solution of the first-order differential equation $\frac{d\Phi_b}{d\tilde{\eta}} = \frac{\hat{v}_b}{\delta_{iz}(\Phi_b)}$ with $\Phi_b(0) = 0$.

3 | EFFECTIVE SXB COEFFICIENT WHEN SPATTERED NEUTRAL IMPURITIES ARE IONIZED WITHIN THE SHEATH REGION

We examine in this section the effects of the ionization of sputtered neutral impurities in the sheath on the SXB coefficient introduced by Behringer^[5] to spectroscopically determine the flux of impurity sputtered from material surface. Effects of metastable states are not included for the sake of simplicity. Following Behringer^[5], the flux of neutral impurity sputtered from a material surface Γ_{ero} can be inferred from the photon flux ϕ_{photon} by the introduction of the SXB coefficient $\frac{S_{iz}}{S_{ph}}$, where S_{ph} is the photon emissivity coefficient, such that

$$\Gamma_{\text{ero}} = \underbrace{\frac{S_{iz,p}}{S_{ph,p}}}_{\text{SXB coefficient}} \times \underbrace{\int_0^\infty S_{ph} n_{\text{imp}}(\hat{z}) n_e(\hat{z}) d\hat{z}}_{\phi_{\text{photon}}}, \quad (10)$$

where $S_{ph,p}$ is the value of S_{ph} at the entrance of the sheath. The measurement of Γ_{ero} using expression (10) relies on the assumption that the SXB coefficient is constant along the field of view above the divertor plate. However, the dependence of S_{iz} and S_{ph} on \hat{z} must be taken into account in the expression of the SXB coefficient when impurities are ionized in the sheath region. In this case, expression (10) is recast into

$$\Gamma_{\text{ero}} = \underbrace{\frac{S_{iz,p}}{S_{ph,p}} \frac{\int_0^\infty \delta_{iz}(\hat{z}) g_{iz}(\hat{z}) d\hat{z}}{\int_0^\infty \delta_{ph}(\hat{z}) g_{iz}(\hat{z}) d\hat{z}}}_{\text{effective SXB coefficient}} \times \phi_{\text{photon}}, \quad (11)$$

where we have introduced δ_{ph} such that $S_{ph}(\hat{z}) = S_{ph,p} n_{e,p} \times \delta_{ph}(\hat{z})$, similarly to expression 4. Expression (11) shows that the effective SXB coefficient is lower than $\frac{S_{iz,p}}{S_{ph,p}}$ when the effects of the variation of the electron distribution in the sheath are stronger on the ionization rate than on the photon emissivity rate ($\delta_{iz} < \delta_{ph}$).

4 | IONIZATION OF SPATTERED NEUTRAL TUNGSTEN IMPURITIES IN PRESENCE OF A CHODURA SHEATH IN DIVERTOR

The ionization of tungsten impurities physically sputtered from divertor PFCs in the presence of a Chodura sheath is considered in this section using the results derived in Section 2. In tokamak divertor, the magnetic field lines intersect the divertor material surfaces at a shallow angle α , usually less than 5° . As a consequence, the charge separation in the sheath occurs a scale length of the order of the main plasma ion Larmor radius ρ_i .^[3] The decay of the electric potential thus occurs on a scale length of several ρ_i , as shown in several recent kinetic simulations,^[9-11] and the sheath width is thus much larger than the Debye length $\lambda_{\text{sheath}} \sim \rho_i \gg \lambda_{\text{Debye}}$. We assume in this work that the profile of the sheath electric potential is given by expression (12) with $\beta_{\text{sheath}} = 4$, obtained from the kinetic simulations performed by Coulette at $\alpha = 2'$.^[9]

$$\hat{\phi}_{\text{sheath}}(\hat{z}) = -\Lambda e^{-\beta_{\text{sheath}} \hat{z}}. \quad (12)$$

The electric potential, displayed in Figure 1b, is here normalized by the electron temperature $\hat{\phi}_{\text{sheath}} = \frac{e\phi_{\text{sheath}}}{k_b T_e}$. The magnitude of the decay of the electric potential is assumed to be about $\Lambda \approx 2.5$.^[9] Following from expression 12, the sheath

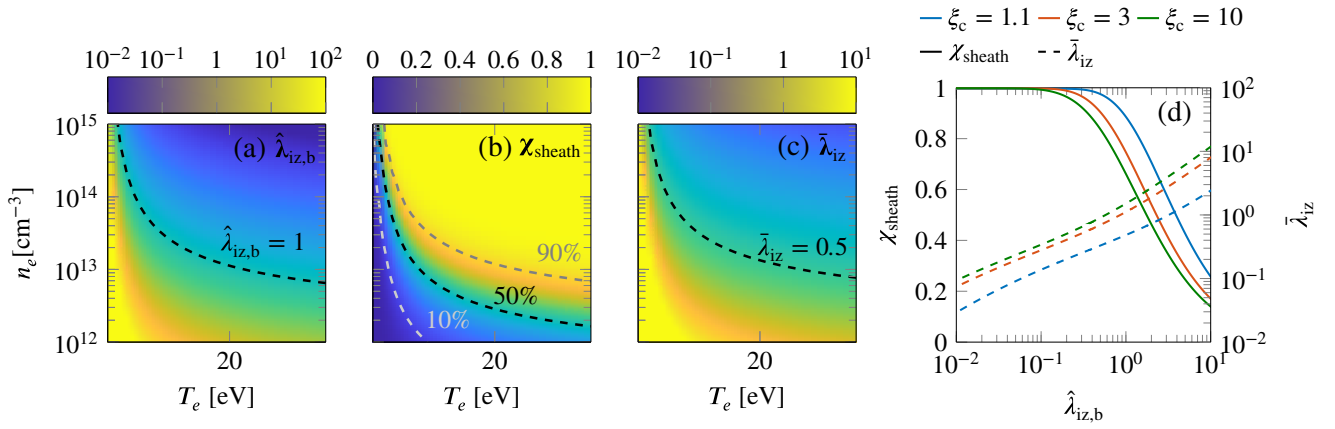


FIGURE 2 Ionization mean-free path of neutral tungsten (a), fraction of neutral tungsten ionizing within the sheath region (b) and average ionization path of neutral tungsten (c) for $\xi_c = 1.5$ as a function of divertor plasma electron temperature and density using tungsten ionization coefficient from the ADAS database.^[12] (d) Fraction of neutral tungsten ionizing within the sheath region χ_{sheath} and average vertical ionization path for neutral tungsten as a function of the ionization mean-free path $\hat{\lambda}_{iz,b}$

width λ_{sheath} is thus formally defined as the distance from the divertor surface above which the difference between the sheath potential and the plasma potential is inferior to 5% ($\hat{\phi}(\hat{z} > 1) < 0.05$). The electron temperature is assumed to be constant in the sheath region, and the electron density in the sheath is assumed to be given by the Boltzmann relationship

$$n_e(\hat{z}) = n_{e,p} e^{\hat{\phi}_{sheath}(\hat{z})}. \quad (13)$$

The ionization coefficients for neutral tungsten are taken from the ADAS database^[12], and they do not exhibit any dependency on the electron density, such that $\delta_{iz}(\hat{z}) = \exp(-\Lambda e^{-\beta_{sheath}\hat{z}})$, and $\int_0^1 \delta_{iz}(\hat{z}) d\hat{z} = 0.59$. The tungsten surface binding energy is assumed to be about $E_b \approx 8.63$ eV.^[13]

The values of the tungsten ionization mean-free path $\hat{\lambda}_{iz,b}$, the fraction of neutral tungsten ionized in the sheath χ_{sheath} and the average tungsten vertical ionization path $\bar{\lambda}_{iz}$ are reported in Figure 2a–c as a function of n_e and T_e for $\xi_c = 1.5$, which corresponds to $E_{cutoff} = 13$ eV. It should be noticed that the distribution of the vertical ionization path g_{iz} for tungsten weakly depends on ξ_c and so do χ_{sheath} and $\bar{\lambda}_{iz}$ (Figure 2d).

In the range of attached divertor plasma conditions expected in ITER and future fusion reactors $n_e \gtrsim 10^{14}$ cm $^{-3}$ and $T_e \gtrsim 5$ eV, a large fraction of sputtered neutral tungsten in divertor are ionized within the sheath region ($\chi_{sheath} \approx 1$). Furthermore, neutral tungsten in these high-density plasma conditions are ionized early in the sheath region where the variation of the electron distribution is large ($\hat{\lambda}_{iz,b} \leq 0.5$). In contrast, only a minority of sputtered tungsten are ionized within the sheath region near the sheath entrance ($\bar{\lambda}_{iz} > 0.5$) in divertor experiments performed at lower divertor plasma density $n_e \lesssim 10^{13}$ cm $^{-3}$.^[14–16]

Consequently, effects of the Chodura sheath on the ionization of tungsten impurity are expected to be significant in high-density divertor plasma ($n_e \gtrsim 5 \times 10^{13}$ cm $^{-3}$) but can be ignored in divertor plasma at lower density, as illustrated in the next section.

5 | EFFECTS OF THE CHODURA SHEATH ON THE SPECTROSCOPIC MEASUREMENTS OF TUNGSTEN GROSS EROSION FLUX IN TOKAMAK DIVERTOR

Effects of the Chodura sheath on the SXB coefficient used to monitor tungsten sputtering in tokamak divertor through the WI line emissions at 400.9 nm^[14,15,17] are analysed in this section using the sheath model and other tungsten parameters introduced in the previous section. However, no photon emissivity coefficient corresponding to this emission line is available in the ADAS database. In lieu of ionization and photon emissivity coefficients from the ADAS database, we consider in this section the ionization coefficient S_{iz} and the photon emissivity coefficient S_{ph} obtained from the collisional radiative model ColRadPy.^[18] These coefficients were derived with an ionization cross section obtained by the exchange

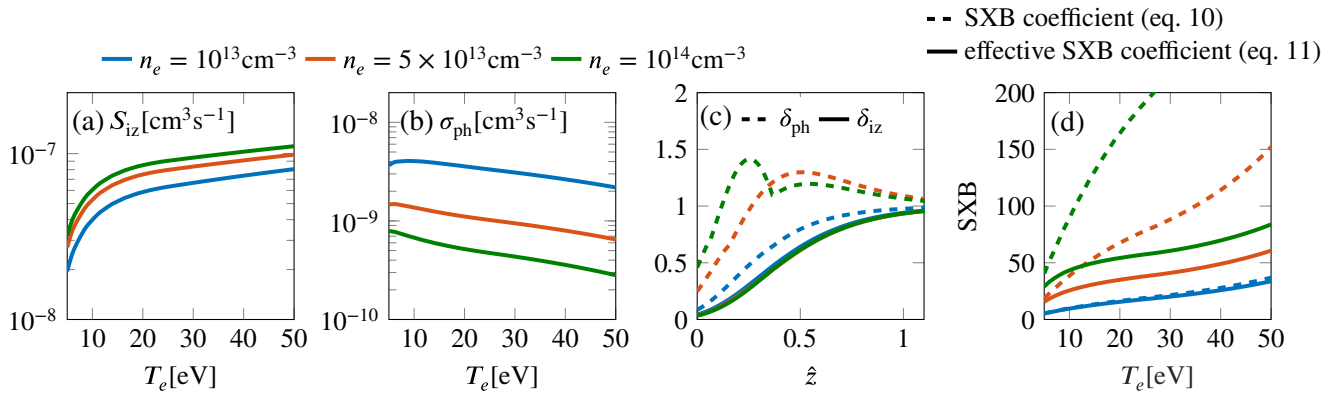


FIGURE 3 Illustration of the effect of the Chodura sheath on the effective SXB coefficient corresponding to the WI line at 400.9 nm (d) calculated using the ionization rate (a) and the photon emission coefficient (b) obtained with the collisional radiative model ColRadPy (see Section 5). The corresponding variations of the ionization rate and the photon emission coefficient in the sheath region are displayed in plot (c)

classical impact parameter method^[19] using the energy structure from a non-perturbative Dirac R-matrix calculation performed by Smyth et al.^[20] to determine the electron impact excitation coefficients.

S_{iz} and S_{ph} exhibit different dependencies on the electron density (Figure 3a, b). Because of the stronger variations of S_{ph} with the electron density, δ_{ph} is larger than δ_{iz} , in particular at high electron density (Figure 3c) for which neutral tungsten are ionized well within the sheath region ($\bar{\lambda}_{iz} < 0.5$). As a result, the effective SXB coefficient given by expression (11) is strongly reduced at high plasma density due to the ionization of tungsten impurities within the sheath region (Figure 3d).

Accurate first-principle modelling of both ionization and photon emissivity coefficients is thus required to calculate SXB coefficients relevant to the spectroscopic measurement of tungsten erosion in divertor operating at high plasma density. It should be pointed out that inaccuracies in S_{iz} and S_{ph} are unlikely to cancel out each other in the expression of the effective SXB coefficient when the effects of the Chodura sheath on tungsten ionization and emission are significant.

6 | SUMMARY

An analytical expression for the distribution of the vertical ionization path of neutral impurities is derived to describe the effects of the electric sheath, induced by the variation of the electron distribution in the sheath region, on the ionization of neutral impurities. The magnitude of these effects can be estimated from the fraction of impurity, which are ionized within the sheath region and the average vertical ionization path relative to the sheath width derived in this work. An expression of the effective SXB coefficient for neutral impurities considering the effects of the variation of the electron distribution in the sheath region on impurity ionization and emission is then obtained.

Using these results, it is shown that the SXB coefficient used to spectroscopically determine the amount of tungsten impurity physically sputtered from divertor plates is significantly reduced due to the ionization of neutral tungsten well within the sheath region in high-density attached divertor plasma conditions ($n_e \gtrsim 5 \times 10^{13} \text{ cm}^{-3}$). For those plasma conditions, accurate modelling and estimation of both ionization and emission rates is critical to estimate the effective SXB coefficient since the variation of the electron distribution in the sheath affects likewise the ionization rate and the emission rate of neutral tungsten.

It should be noticed that the model introduced in this work to describe the ionization and emission of physically sputtered neutral impurities within the sheath accounts for the variations of the electron distribution in the sheath without any assumption about the electron density and temperature. Therefore, this model can be straightforwardly applied to consider kinetic effects in the electron distribution, for example, variation of the electron temperature in the sheath, energetic electron component in the tail of the electron distribution, and so on. Finally, the derivation of the present model should be extended, for instance within the framework of the generalized collisional radiative model ColRadPy,^[18] to take into consideration tungsten metastable states which may significantly affect tungsten ionization and emission at low plasma density.

ACKNOWLEDGMENTS

This material is based upon work supported by the U.S. Department of Energy, Office of Science, Office of Fusion Energy Sciences under Awards DE-SC0018423 and DE-FG02-95ER54309.

CONFLICT OF INTEREST

This report was prepared as an account of work sponsored by an agency of the United States Government. Neither the United States Government nor any agency thereof, nor any of their employees, makes any warranty, express or implied, or assumes any legal liability or responsibility for the accuracy, completeness, or usefulness of any information, apparatus, product, or process disclosed, or represents that its use would not infringe privately owned rights. Reference herein to any specific commercial product, process, or service by trade name, trademark, manufacturer, or otherwise does not necessarily constitute or imply its endorsement, recommendation, or favouring by the United States Government or any agency thereof. The views and opinions of authors expressed herein do not necessarily state or reflect those of the United States Government or any agency thereof.

REFERENCES

- [1] R. Pitts, S. Carpentier, F. Escourbiac, T. Hirai, V. Komarov, S. Lisgo, A. Kukushkin, A. Loarte, M. Merola, A. S. Naik, R. Mitteau, M. Sugihara, B. Bazylev, P. Stangeby, *J. Nucl. Mater.* **2013**, 438, 48.
- [2] R. Chodura, *Plasma-wall transition in an oblique magnetic field. The Phys. Fluids* **1982**, 25(9), 1628–1633.
- [3] D. D. Ryutov, *Contrib. Plasma Phys.* **1996**, 36(2–3), 207.
- [4] G. Fussmann, W. Engelhardt, D. Naujoks, K. Asmussen, S. Deschka, A. Field, J. C. Fuchs, C. Garcia-Rosales, S. Hirsch, P. Ignacz, et al., in *Proc. 15th Int. Symp. Plasma Physics and Controlled Nuclear Fusion Research*, **1995**, pp. 143.
- [5] K. Behringer, H. P. Summers, B. Denne, M. Forrest, M. Stamp, *Plasma Phys. Controlled Fusion* **1989**, 31, 2059.
- [6] M. W. Thompson, *Philos. Mag.* **1968**, 18(152), 377.
- [7] M. A. Lieberman, A. J. Lichtenberg, *Principles of Plasma Discharges and Materials Processing*, John Wiley & Sons, **2005**.
- [8] M. Abramowitz, I. A. Stegun, *1965*, *Handbook of Mathematical Functions: with Formulas, Graphs, and Mathematical Tables*, National Bureau of Standards, Applied Mathematics Series. Vol. 55, Hoboken, NJ: Courier Corporation, **1977**.
- [9] D. Coulette, G. Manfredi, *Plasma Phys. Controlled Fusion* **2016**, 58, 025008.
- [10] D. Tskhakaya, M. Groth, *J. Nucl. Mater.* **2015**, 463, 624.
- [11] I. Borodkina, D. Borodin, A. Kirschner, I. Tsvetkov, V. Kurnaev, M. Komm, R. Dejarnac, JET Contributors, *Contrib. Plasma Phys.* **2016**, 56(6–8), 640.
- [12] H. P. Summers, *The ADAS user manual, version 2.6*, **2004**, (file scd50_w.dat). <http://www.adas.ac.uk> (accessed: June 2019).
- [13] W. Eckstein, J. Roth, *Nucl. Instrum. Methods Phys. Res. Sect. B: Beam Interact. Mater. Atoms* **1991**, 53(3), 279.
- [14] T. Abrams, R. Ding, H. Y. Guo, D. M. Thomas, C. P. Chrobak, D. L. Rudakov, A. G. McLean, E. A. Unterberg, A. R. Briesemeister, P. C. Stangeby, J. D. Elder, W. R. Wampler, J. G. Watkins, *Nucl. Fusion* **2017**, 57, 056034.
- [15] S. Brezinsek, D. Borodin, J. W. Coenen, D. Kondratjew, M. Laengner, A. Pospieszczyk, U. Samm, *Phys. Scr.* **2011**, T145, 014016.
- [16] M. Laengner, S. Brezinsek, J. Coenen, A. Pospieszczyk, D. Kondratyev, D. Borodin, H. Stoschus, O. Schmitz, V. Philipps, U. Samm, *J. Nucl. Mater.* **2013**, 438, S865.
- [17] G. J. van Rooij, J. W. Coenen, L. Aho-Mantila, S. Brezinsek, M. Clever, R. Dux, M. Groth, K. Krieger, S. Marsen, G. F. Matthews, A. Meigs, R. Neu, S. Potzel, T. Putterich, J. Rapp, M. F. Stamp, *J. Nucl. Mater.* **2013**, 438, 42.
- [18] C. A. Johnson, S. D. Loch, D. A. Ennis, *Nucl. Mater. Energy* **2019**, 100579.
- [19] A. Burgess, H. P. Summers, *Mon. Not. R. Astron. Soc.* **1976**, 174(2), 345.
- [20] R. T. Smyth, C. P. Ballance, C. A. Ramsbottom, C. A. Johnson, D. A. Ennis, S. D. Loch, *Phys. Rev. A* **2018**, 052705, 1.

SUPPORTING INFORMATION

Additional supporting information may be found online in the Supporting Information section at the end of this article.

How to cite this article: Guterl J, Johnson C, Ennis D, Loche S, Snyder P. Effects of the Chodura sheath on tungsten ionization and emission in tokamak divertors. *Contributions to Plasma Physics*. 2019;e201900140. <https://doi.org/10.1002/ctpp.201900140>